PERGAMON

Solid State Communications 122 (2002) 445–450

solid state communications

www.elsevier.com/locate/ssc

Recent studies on In_2S_3 containing oxygen thin films

N. Barreau[a], J.C. Bernède[a,*], H. El Maliki[a], S. Marsillac[a], X. Castel[b], J. Pinel[b]

[a]*LPSE-FSTN, Equipe couches minces et materiaux nouveaux, Universite de Nantes, 2, Rue de la Houssinière, BP 92208, 44322 Nantes Cedex 3, France*

[b]*URER, Groupe de Microélectronique et Visualisation, Université de Rennes I, Campus de Beaulieu, 35042 Rennes Cedex, France*

Received 21 June 2001; received in revised form 4 February 2002; accepted 13 February 2002 by P. Burlet

Abstract

Attention has recently been paid to In_2S_3 thin films because of their potential application as buffer layer in CIGS-based solar cells. In this paper, the recent studies performed on such thin films deposited by chemical bath deposition (CBD) and physical vacuum deposition (PVD) are reported and compared. The main part of the experimental results exposed concerns the wide band gap PVD deposited β-In_2S_3 thin films. The influence of the synthesis conditions on the physico-chemical, optical, and electrical properties are reported and discussed in the paper. The oxygen present in the CBD and PVD films has been found to be the origin of their optical properties, which make them a good candidate to substitute CdS in thin films solar cells as buffer layer. The films have a n-type electrical conductivity and their optical band gap is about 2.8 eV.

PACS: 71.20.Nr; 74.25.Gz; 78.20. − e

Keywords: A. Indium sulphide; A. Thin films; D. Optical properties; D. Structural properties

1. Introduction

Chalcogenide based solar cells with high efficiencies (>17%) have been achieved by several groups [1–3]. The absorbing layer in these devices is a p-Cu(In,Ga)Se_2 of about 2–3 μm thickness, which is crystallized in the chalcopyrite structure. This film is obtained by either co-evaporation or selenization of metal layers sequentially evaporated. The junction necessary for the occurrence of the photovoltaic effect is typically fabricated using a CdS buffer layer deposited by chemical bath deposition (CBD). Not only these films are n-type but also quite resistive, which allows to avoid the formation of shunt path between the Mo under electrode and the transparent conductive oxide of the upper electrode. If the use of CdS is very efficient in achieving performing cells, it is undesirable from the environmental safety point of view because of the cadmium. Moreover, its band gap value (2.48 eV) induces some optical absorption loss at short wavelengths. Therefore, the research of a wider band gap semiconductor without cadmium, involves the effort of many research teams [4–7]. Some very promising results have been obtained with ZnS deposited by CBD [6]. However, the CBD technique itself constitutes a bottleneck in the deposition process and a whole process using only physical vacuum deposition (PVD) technique should be, finely, preferable for industrial development.

In the present paper we have focused our interest on a n-type semiconductor thin film, which can be synthesized either by CBD or PVD, the β-In_2S_3 containing oxygen. This material corresponds to the specification of a good solar cell buffer layer. More specifically, many works have been reported on CBD-In_2S_3 [2,8,9]. In this work, the ability to grow In_2S_3 thin films by CVD and PVD techniques is demonstrated and their properties are compared. Since many works have not been reported on the PVD technique we mainly focus our interest on the PVD films.

2. Experimental

2.1. Deposition technique

In order to compare the quality of the different films, we have deposited In_2S_3 by CBD and PVD.

* Corresponding author. Tel.: +33-2-51-12-55-30; fax: +33-2-51-12-55-28.

E-mail address: jean-christian.bernede@physique.univ-nantes.fr (J.C. Bernède).

0038-1098/02/$ - see front matter
PII: S0038-1098(02)00099-6

2.1.1. Chemical bath deposition conditions

In_2S_3 thin films were grown by CBD on SnO_2 coated or bare soda lime glass substrates. SnO_2 (TCO) films were provided by SOLEMS. The substrate were sonicated in alcohol and rinsed in boiling distilled water. The CBD-In_2S_3 films were grown in a thermostated bath whose temperature was 345 K. The substrates were clamped vertically with plastic clamps and kept immersed in the stirred solution. The deposition takes place in a aqueous solution containing indium(III) chloride ($[InCl_3] = 0.01$ mol l^{-1}) and thioacetamide ($[CH_3CSNH_2] = 0.15$ mol l^{-1}). After deposition, the samples were removed from the bath and sonically washed in distilled water until heterogeneities are removed. Then they were dried in air.

2.1.2. Physical vapor deposition process

Thin film obtention process: the technique used will only be shortly recalled since it has already been described elsewhere [10,11].

The thin film obtention process can be divided into two steps, the deposition of the constituents onto substrates and the post-deposition annealing in flowing argon of the samples evaporated.

The deposition of the constituents is carried out by vacuum thermal evaporation, at a gas pressure of 5×10^{-4} Pa, using a tungsten crucible for indium and a 'Laboratory made' Pyrex crucible for the sulfur. The purities of indium and sulfur used are 99.99 and 99.98%, respectively. The films were deposited on soda lime glasses. All the substrates were cleaned chemically before evaporation. In order to obtain the films, thin indium and sulfur layers were sequentially deposited, their thickness and evaporation rate being controlled in situ by an hf quartz monitor. The thickness ratio has been experimentally determined to finally have homogenous films with an atomic ratio at.%S/at.%In ≥ 3.

The structures obtained from this process were then annealed in a tubular oven for 30 min under a constant argon flow of 0.6 dm^3 min^{-1}. The films have been annealed at five different temperatures 523, 573, 623, 673, and 723 K. The heating time and the temperature rate increase have been varied as discussed in the manuscript. The samples studied in this paper were about 100 nm thick.

2.2. Experimental characterization

The obtained films were analyzed by X-ray diffraction (XRD) to investigate the compound and structure formation; a Siemens X-ray goniometer with Cu Kα line was used in the study.

For observing the surface and cross-section morphology of the films, a JEOL-type JSM 6400F scanning electron microscope (SEM) was used.[1]

The surface and depth profiling composition (quantitative and qualitative) of the films were obtained from X-ray photoelectron spectroscopy (XPS) measurements.[2] Electron micropobe analysis (PGT-IMIX PTS model) was used to determine the chemical composition of the films.[1]

The optical measurements were done at room temperature using a spectrophotometer CARY and the transmittance is measured in the wavelength interval of 300–800 nm.[3]

Infra red spectra were recorded on Perkin Elmer 1600 Fourier transform infrared (FTIR) spectrometer in the range 400–4000 cm^{-1}. The resolution of the instrument was 4 cm^{-1}.

3. Experimental results

Since CBD-In_2S_3 films have been already studied [12,13], the main part of the experimental works concerns the PVD process, while results obtained on CBD films are presented at the end of this section.

3.1. PVD-In_2S_3 films

The films obtained from the PVD process have been synthesized in two steps. The first one is the deposition of the films by thermal evaporation and the second is the post-deposition annealing.

As described earlier, the synthesis process of the PVD deposited thin films consists in the annealing, under constant argon flow, of structures composed of thin layers of indium and sulfur superposed. The properties of the thin films obtained have been found to strongly depend on the annealing conditions; therefore, the annealing temperature and duration have been used as parameters. The influence of the temperature rate increase has also been studied.

At first, it must be specified that, whatever may be the experimental conditions used in the present work, all the films have a n-type conductivity. Moreover, it has been shown by SEM [11] that the films are very homogeneous and their coverage efficiency is excellent.

For the first approach the annealing duration, with reference to earlier works, has been chosen to be half an hour [14].

The annealing temperature has been shown [11] very important in the crystalline properties of the films. This temperature has been varied in steps of 50 K between 523 and 723 K. The XRD diagram obtained from each film are shown in Fig. 1. It can be seen that there is a 'threshold' temperature at 623 K. Below this temperature the crystallization is only initialized while above this temperature the films are wholly crystallized in the quadratic structure of β-In_2S_3 (JCPDS Data 25-390), and only the grain size varies. It can be observed that this threshold concerns not only the crystalline properties of the films, but also their

[1] Service commun de microscopie electronique à balayage et de microanalyse de l'Université de Nantes.

[2] Université de Nantes—CNRS.

[3] Laboratoire de Physique Cristalline—IMN.

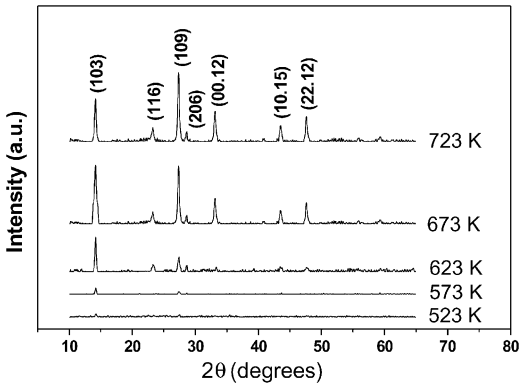

Fig. 1. XRD diagrams of PVD-In_2S_3 thin films synthesized at 523, 573, 623, 673, and 723 K.

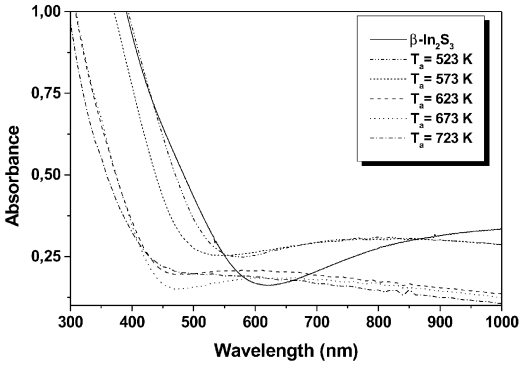

Fig. 2. Evolution of the optical absorbance versus the wavelength of the PVD-films annealed at different temperatures, T_a, and of films of pure β-In_2S_3.

optical properties. Fig. 2 shows the evolution of the absorbance of a pure β-In_2S_3 thin film, the increase in the optical band gap of PVD films with the annealing temperature until it is 623 K, whereas for higher annealing temperatures absorption threshold is stable.

The composition of the films has been studied by EMPA and XPS before and after annealing. As far as the results of the EMPA study on the annealed films are concerned, the atomic ratio of sulfur and indium (Fig. 7) has only been studied because the thin thickness of the films (100 nm) induces the detection of the elements of the substrate, which disturbs the quantification of oxygen and sodium.

The quantitative XPS analyses have shown that the films after annealing contain oxygen and that there is some sodium not only at the surface but also in the bulk of the films. It should be observed that before annealing, there is neither oxygen nor sodium contamination of the films, while there is some excess sulfur present. We have performed some more characterizations of these unheated samples. The visualization of the cross-section (in the back scattered mode) of the films before annealing testify clearly that even if, as shown by the XRD diagrams, the films are amorphous, there is an 'intimate' interdiffusion between the In and S sequentially deposited layers (not shown). There is not only a physical interdiffusion but also a chemical interaction between indium and sulfur as shown by XPS (Fig. 3(a)). The XPS analyses allow the study of the chemical state of different elements. If the binding energy of the In 3d peak is not highly sensitive to the binding state of indium atom, that of sulfur testifies clearly that even before annealing there is, at least, a partial bond formation between S and In. The binding energy of the S 2p ray is indeed 162 eV in In_2S_3 [15] while it is 164 eV [16] for sulfur alone. The XPS depth profile has confirmed the In and S interdiffusion. It should be also noted that the oxygen present at the surface of the film is not bonded to indium (530 eV) or sulfur (there is no sulfur oxide peak), but it is only present as a contaminant physically adsorbed (Fig. 3(b)) (535 eV) [16].

After annealing, as shown earlier, there is some oxygen and sodium contamination of the films. The difference between the oxygen involved in surface contamination and that introduced in the films during annealing is clearly shown in Fig. 4. After annealing the main part of the oxygen, in the films, corresponds to oxygen bonded to indium. This contribution increases relatively after surface etching, which eliminates preferentially weakly bonded atoms, i.e. contamination. The increase in annealing temperature increases the crystalline properties of the films. However, above 673 K, there is a saturation effect, while the Na and O superficial concentration increases strongly. Therefore, it appears that the optimum annealing temperature, T_a, is 673 K. So we have proceeded to different annealing at $T_a = 673$ K, using the annealing time or the temperature rate increase as parameter. In the first case, the annealing time, t_a, was varied between 0 and 45 min, the heating rate being 4.4 K min^{-1}, i.e. the time necessary to achieve T_a was 90 min, while the cooling time was 150 min. The thickness of all the films being the same, the physico-chemical characterization of these samples shows that the XRD spectra are similar (Ipeak, FWHM), the results of the quantitative analysis are also similar with a small sulfur deficiency as usually observed in the films, the micrographs of the surface are also alike, and more surprising, the band gap also.

When the heating rate is used as a parameter, with $T_a = 673$ K, $t_a = 30$ min, the main new information is obtained with transmission measurements. Fig. 5 shows that when the heating rate decreases, mainly from 6.7 to 4.4 K min^{-1} there is a blue shift of the absorption threshold.

We have also proceeded to some IR absorption measurements and the presence of hydroxyl radicals in the films after annealing is probable, as shown in Fig. 6.

3.2. CBD films

The films are about 30–50 nm thick after a deposition time of about 25 min and are amorphous. XPS measurements have been performed on such samples. They have

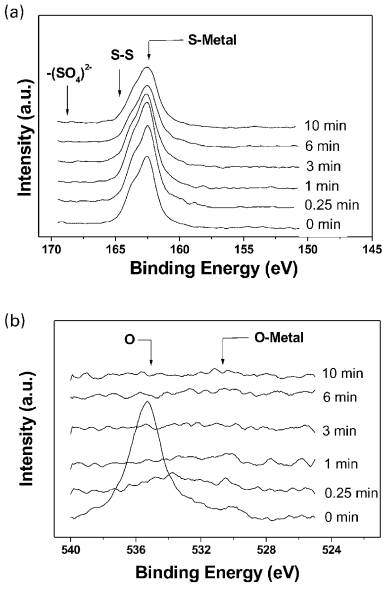

Fig. 3. (a) Evolution of the S 2p peak with the etching time of a PVD-film before annealing. (b) Evolution of the O 1s peak with the etching time of a PVD-film before annealing.

shown that, after an etching of 1 min, in order to avoid the surface contamination, there is 37 at.% of In, 18 at.% of S, and 45 at.% of O, i.e. we have nearly $In_2(S_x,O_y)_3$. It should be observed that, here also, the main contribution of the oxygen corresponds to In–O bonds. The presence of the OH is attested by IR measurements. The optical band gap of these films, which are n-type, has also been measured to be about 2.90 eV.

All the obtained results and those reported in the literature clearly show that CBD In_2S_3 films do not correspond to pure In_2S_3. There is possibly a mixture of oxide and hydroxyl but is difficult to attribute clearly the signal to either contribution.

4. Discussion

First of all we will describe the reaction process involved in the growth of the PVD In_2S_3 films, then the influence of oxygen/hydroxyl on the optical properties of the In_2S_3 films will be discussed and finally some interpretation on the variation of the electrical properties with the temperature of annealing, T_a, will be proposed.

Before annealing, it has been shown that there is some initialization of the In–S chemical reaction. However, the films are amorphous, they contain a large amount of excess sulfur. Therefore, the films consist in In–S bonds randomly distributed in an amorphous sulfur matrix. The density of dangling bonds and defaults is very high in such heterogeneous materials. It should be noted that the vapor pressure of sulfur is very high, 1 Pa at 606 K and 10 Pa at 739 K, and there will be some sulfur escape during annealing under pressure atmosphere.

The argon used during the annealing is the argon Nertal (O_2: 3 ppm, H_2O: 3 ppm), i.e. there is a small oxygen contaminant pressure during the crystallization process. It should be also noted that the 'free enthalpy' of In_2O_3 is $-957\ kJ\ mol^{-1}$, while that of In_2S_3 is $-414\ kJ\ mol^{-1}$ at 298 K [17].

Therefore, there is a competition between sulfur escape from the film, and sulfur and oxygen reactivity with indium. The overall process is controlled, not only by thermodynamics but also by chemical kinetics.

Before any interpretation, it is very informative to plot the evolution of the atomic ratio of S/In with the annealing temperature. Fig. 7 shows that the shape of the two curves obtained from EMPA and XPS is the same, there is only a translation effect related to the fact that XPS measurements, in order to avoid surface contamination effect, have been performed after 1 min of etching, which minimizes the S atomic concentration as its etching rate is higher than that of indium.

When the annealing temperature, T_a, is smaller than 623 K, the oxygen contamination is small, however, as shown by XRD the films are poorly crystallized i.e. many In–S bonds are weak, and the sulfur escape from the film is important and overpass the expected boundary corresponding to In_2S_3. At the end of the annealing process, we have β-In_2S_3 poorly crystallized films slightly contaminated with oxygen.

When the annealing temperature increases up to 623 K, the crystalline properties of the films increase, i.e. the chemical reaction between the constituents is stronger, the In–S bonds are stable and the atomic ratio of S/In increases. At the same time, since the heating temperature is higher, the oxygen reactivity increases and the oxygen contamination is higher. The sodium contamination, which originates from the soda lime glass substrate increases. This last phenomenon has been described earlier in the case of ternary chalcopyrites such as $CuInSe_2$ [18,19]. However, it should be noted that presently the sodium remains all over the thickness of the films, while it accumulates at the surface in the case of the ternary compounds.

We have shown that probably some hydroxyl radicals are bonded to indium in the films. Contrarily to oxygen, which can be substituted by sulfur is a In_2S_3 crystalline, the OH bonds stop the crystallite growth. This effect can explain that when T_a is increased above 673 K there is no improvement in the crystallization of the films, although the grains remain quite small (<100 nm). The only effect of the increase in temperature is an increase in the oxygen contamination, mainly at the surface of the films.

The growth of CBD films is not discussed here since it has been extensively studied by other authors [2,8,12,13].

After the discussion of the crystallization process, some proposition could be performed to explain the band gap value of the films. First of all, it should be noted that the band gap value of β-In_2S_3 is 2 eV [20]. As far as the PVD β-In_2S_3 films are concerned, the values deduced from the

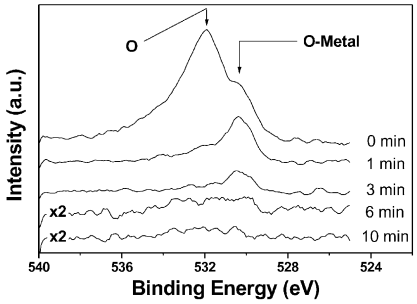

Fig. 4. Evolution of the O 1s peak with the etching time of a PVD-film after annealing.

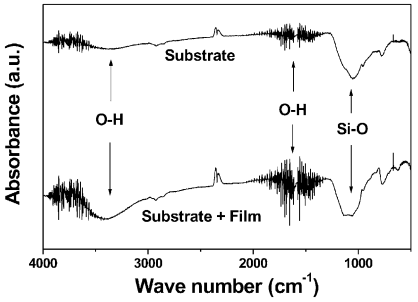

Fig. 6. IR absorption spectrum of a PVD-In_2S_3 film and of its naked substrate for comparison.

transmittance are about 2.9 eV [21]. It can be observed that, when oxygen is introduced into the films, the band gap values are far higher than that of the single crystals. In the case of CBD thin films, systematically broadened gaps (>2.8 eV) are obtained.

Many studies have been made on CBD-In_2S_3 films, they have shown that the deposited films are in fact indium hydroxyl sulfide thin films. The XPS studies of these films [13] show that there is some oxygen and some hydroxyl bonded to indium. The CBD films are sulfur deficient and there are more oxygens than sulfurs in the films, with this oxygen compensating the sulfur deficiency. Therefore, XPS characterization proves that films are mainly composed of indium hydroxyl sulfide, indium oxide, and indium sulfide. The difficulty is that the amount of hydroxide ion could vary strongly from one sample to another without any coherent relation to the deposition conditions.

When the PVD films are concerned, different contributions can be invoked to justify the broadening effect of the band gap. Some authors have invoked a grain size effect [22]. A blue shift effect of the optical properties can be induced by very small grain size. As discussed by Yoshida et al. [23], to be significant the grain size should be 8 nm or less, while the grain size of our film estimated from the FWHM of the XRD peak and visualized by SEM is about 20–30 nm, therefore such quantization effect should be very small in our films.

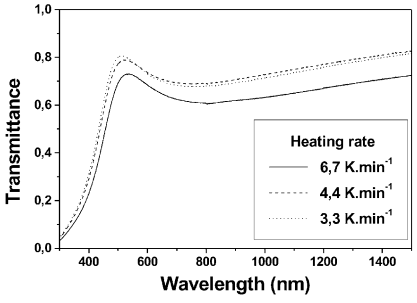

Fig. 5. Evolution of the optical transmittance of PVD-films annealed during 30 min at 673 K, the temperature rate increase being 3.3, 4.4, and 6.7 K min^{-1}.

Some others attribute the gap broadening to excess sulfur [24] but our films are sulfur deficient. Since it has been shown that some In–O bands are present in the films, the films can behave like an alloy as described by Hill [25].

If A and B are two semiconductor compounds, the gap variation, when xA is present in $(1-x)$B, is given, in the case of often used linear model, by:

$$Y = E_B - (E_B - E_A)x \quad (1)$$

where $E_B = E_{gIn_2S_3} = 2.1$ eV optical band gap value of In_2S_3, $E_A = E_{gIn_2O_3} = 3.5$ eV optical band gap value of In_2O_3, Y optical band gap value of the alloy $A_xB_{(1-x)}$.

Using Eq. (1), even if the most favorable condition is taken with $x = 0.1$, the value calculated is $Y \approx 2.24$ eV. This value is far smaller than those obtained experimentally.

Hill [25] has shown that it is usual to describe the energy gap of an alloy A_xB_{1-x} in terms of pure compound energy gap E_A and E_B as:

$$E_{(x)} = E_B + (E_A - E_B - b)x + bx^2 \quad (2)$$

where b is the bowing parameter which induces a difference between the linear average. If the linear evolution is noted E_{lin} and the evolution with the bowing parameter is noted E_{Hill}, the difference ΔE between these two evolutions is $\Delta E = E_{lin} - E_{Hill} = bx - bx^2$. As $b \geq 0$ and $x \in [0;1]$, the difference ΔE is always negative. Therefore, this

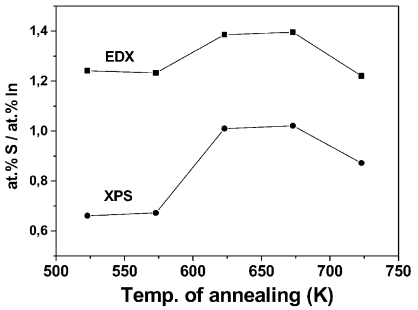

Fig. 7. Variation of the atomic ratio S/In in the PVD-In_2S_3 films with their annealing temperature.

evolution, which is under linear, cannot a fortiori explains totally the anomalously broad optical band gap of our In_2S_3 compounds, and hence another contribution should be taken into account. We have shown that not only oxygen but also Na is present in the films. The substitution of indium by sodium in the In_2S_3 films should increase also the band gap [26], however, EMPA study has shown that the atomic ratio %In/(%S + %O) is about 0.66. For the β-In_2S_3 crystallizing under a defect spinel form, one can think that sodium could be intercalated in the cation vacancies, however, such a compound has never been found.

When the CBD-In_2S_3 films are concerned, the oxygen and hydroxyl contents are far higher to justify the value of the gap. In the case of PVD films, if all the effects discussed earlier can contribute to the gap broadening, the oxygen atomic percentage is too small and the grain size too large to justify the broadening effect alone.

Calculations have been performed using a scalar-relativistic version of the *k*-space TBLMTO model with the atomic-sphere approximation (ASA). The simulation of oxygen introduction in the β-In_2S_3 structure shows that the oxygen states are not located near the band gap, however oxygen/hydroxyl can modify the crystal field with crystal structure distortions and small sulfur position variations. Such perturbations have been proved to induce large band gap increasing in the case of other sulfur compounds and calculations introducing such small deviations on the sulfur bond length are under way, and therefore this new and exciting fundamental field remains open [27].

If we compare the CBD samples to the PVD films, the oxygen and hydroxyl contamination is smaller in the second case, while the band gap values are similar. The major difference between the two kinds of films consists in their crystalline properties, the crystallinity of PVD films is far better than that of CBD. The crystal field of the first must be more perturbed than the latter, which can explain the greater influence of oxygen substituted by sulfur on the electronic structure of the material. In addition to oxygen contaminants, there is also sodium in the PVD films. The influence of such impurity on the optical band gap of materials has never been reported in the literature and is actually studied in our laboratory.

The predominance of the heating rate on the properties of the films is clearly shown in Fig. 7, while the influence of the annealing duration is small [21]. When heating rate increases, the gap is not as broad as discussed earlier because of the fast crystallization. For a given heating rate, the heating time itself in not important. When the heating rate is quick enough, the In–S bonds are consolidated rapidly, before all the excess sulfur escapes, which will prevent large oxygen contamination and the band gap is smaller. When T_a is achieved, the bonds are stabilized, the oxygen contamination does not increase and the band gap is stable.

5. Conclusion

We have shown that by using appropriate annealing conditions PVD-In_2S_3 films can be grown with similar properties to that of CBD-In_2S_3 films. They have n-type conductivity, strong adherence to the substrate, high coverage efficiency and a gap value of about 2.8–2.9 eV. Therefore, they can be used as buffer layer in a whole PVD process of thin film solar cells. More generally it is very important to understand, that, in the present films, the oxygen contamination has a positive effect on properties of the film, to obtain layers with properties, which match very well with the specifications of solar cell buffer layers. Therefore, sometimes, it is important going off the beaten tracks of the knowledge which states that purity is a guarantee for performing layer.

References

[1] H.W. Schock, F. Pfistterer, Renewable Energy World March–April (2001) 75.
[2] L. Stolt, et al., 13th European Photovoltaic Solar Energy Conference, 23–27 October, 1995, p. 1451.
[3] M.A. Contreras, et al., Progr. Photov. Res. Appl. 7 (1999) 311.
[4] A. Ennaoui, et al., Solar Energy Mater. Solar Cells 67 (2001) 31.
[5] K. Kushiya, et al., Solar Energy Mater. Solar Cells 67 (2001) 11.
[6] T. Nakada, et al., Solar Energy Mater. Solar Cells 67 (2001) 255.
[7] A. Shimizu, et al., Thin Solid Films 361–362 (2000) 193.
[8] D. Hariskos, et al., Solar Energy Mater. Solar Cells 41/42 (1996) 345.
[9] D. Braunger, et al., Solar Energy Mater. Solar Cells 40 (1996) 97.
[10] J.C. Bernède, N. Barreau, French Patent No. 7322.
[11] N. Barreau, et al., Vacuum 56 (2000) 101.
[12] C.D. Lockhande, et al., Thin Solid Films 340 (1999) 18.
[13] R. Bayon, et al., Thin Solid Films 353 (1999) 100.
[14] E. Gourmelon, et al., Vacuum 48 (1997) 509.
[15] S.-H. Yu, et al., J. Am. Ceram. Soc. 82 (2) (1999) 457.
[16] J.F. Moulder, et al., Handbook of X-ray Photoelectron Spectroscopy, J. Chastain (Ed.), Perkin-Elmer Corporation, 1992, Minnesota, USA.
[17] J.F. Guillemoles, Thin Solid Films 361–362 (2000) 338.
[18] A. Rockett, et al., Thin Solid Films 372 (2000) 212.
[19] D. Braunger, et al., Thin Solid Films 361–362 (2000) 161.
[20] W. Rehwald, G. Harbeke, J. Phys. Chem. Solids 26 (1965) 1309.
[21] N. Barreau, et al., Phys. Status Solidi A 184 (1) (2001) 179.
[22] E.B. Yousfi, et al., Thin Solid Films 361–362 (2000) 183.
[23] T. Yoshida, et al., Electrochem. Soc. Proc. 97–20 (1997) 37.
[24] W.-T. Kim, C.-D. Kim, J. Appl. Phys. 60 (7) (1986) 2631.
[25] R. Hill, J. Phys. C: Solid State Phys. 7 (1974) 521.
[26] R. Mauricot, Thesis of Doctorat, University of Nantes (France), ISITEM, 1995.
[27] R. Robles, et al., Opt. Mater. (2001).